Journal of Hazardous Materials 199–200 (2012) 247–254

Contents lists available at SciVerse ScienceDirect

Journal of Hazardous Materials

journal homepage: www.elsevier.com/locate/jhazmat

The contribution of vanadium and titanium on improving methylene blue decolorization through heterogeneous UV-Fenton reaction catalyzed by their co-doped magnetite

Xiaoliang Liang[a,b], Yuanhong Zhong[a,b], Sanyuan Zhu[a], Lingya Ma[a,b], Peng Yuan[a], Jianxi Zhu[a], Hongping He[a,*], Zheng Jiang[c]

[a] Key Laboratory of Mineralogy and Metallogeny, Guangzhou Institute of Geochemistry, Chinese Academy of Sciences, Guangzhou 510640, China
[b] Graduate University of the Chinese Academy of Sciences, Beijing 100049, China
[c] SSRF, Shanghai Institute of Applied Physics, Chinese Academy of Sciences, Shanghai 201800, China

ARTICLE INFO

Article history:
Received 27 May 2011
Received in revised form
20 September 2011
Accepted 2 November 2011
Available online 9 November 2011

Keywords:
Magnetite
Isomorphic substitution
XANES
Adsorption
Photo-Fenton

ABSTRACT

This study investigated the methylene blue (MB) decolorization through heterogeneous UV-Fenton reaction catalyzed by V-Ti co-doped magnetites, with emphasis on comparing the contribution of V and Ti cations on improving the adsorption and catalytic activity of magnetite. In the well crystallized spinel structure, both Ti^{4+} and V^{3+} occupied the octahedral sites. Ti^{4+} showed a more obvious effect on increasing specific surface area and superficial hydroxyl amount than V^{3+} did, resulting in a significant improvement of the adsorption ability of magnetite to MB. The UV introduction greatly accelerated MB degradation. And magnetite with more Ti and less V displayed better catalytic activity in MB degradation through heterogeneous UV-Fenton reaction. The transformation of degradation products and individual contribution from vanadium and titanium on improving adsorption and catalytic activity of magnetite were also investigated. These new insights are of high importance for well understanding the interface interaction between contaminants and metal doped magnetites, and the environmental application of natural and synthetic magnetites.

1. Introduction

In recent years, metal-substituted magnetites have attracted great interests in the fields of mineralogy [1], environmental engineering [2] and material science [3]. Especially in environmental engineering, the incorporation of transition metals into magnetite, such as Mn, Cr and Co, can greatly increase the heterogeneous Fenton catalytic activity of magnetite with high efficiency and easy recycle in wastewater purification, e.g. printing and dyeing water [4,5] and wastewater containing persistent organics [6]. Metal-substituted magnetites have been considered as an outstanding candidate of catalysts in advanced oxidation processes (AOPs). The incorporation of Ti also can improve the reductive reactivity of magnetite in radioactive wastewater treatment [7]. It is well known that isomorphous substitution of Fe by transition metals extensively exists in natural magnetites and these magnetites are widely distributed on the earth surface [8]. Thus, magnetites are not only promising catalysts in pollution treatment engineering but also vital geocatalysts in controlling the transportation and transformation of pollutants on the earth surface.

In previous researches, the catalytic activity of metal-substituted magnetite has been comprehensively investigated in terms of species, valence and occupancy of substituting metals. It has been established that substituting metals exhibiting thermodynamically favorable redox pairs (e.g. Mn^{2+}/Mn^{3+} and Co^{2+}/Co^{3+}) can remarkably enhance the catalytic activity of magnetite in H_2O_2 decomposition and organic oxidation [5,9]. The octahedral sites are almost exclusively exposed at the surface of the spinel crystallites and the catalytic activity is mainly due to octahedral cations [10]. Beyond all doubts, these experimental evidences are favorable for the application of metal-substituted magnetites in environmental engineering.

Unfortunately, almost all the previously published researches focused on single-metal-substituted magnetite. In fact, in most natural cases, more than two kinds of metals are simultaneously introduced into magnetites in geological processes [11]. But few studies have been conducted about the influence of co-substituting metals on the structure and properties of magnetite, especially the surface reactivity and catalytic activity. These are critical factors

* Corresponding author. Present address: Key Laboratory of Mineralogy and Metallogeny, Guangzhou Institute of Geochemistry, Chinese Academy of Sciences, 511 Kehua Street, Guangzhou, 510640, China. Tel.: +86 20 85290257; fax: +86 20 85290708.
E-mail address: hehp@gig.ac.cn (H. He).

0304-3894/$ – see front matter © 2011 Elsevier B.V. All rights reserved.
doi:10.1016/j.jhazmat.2011.11.007

for environmental application of natural magnetite. For example, in Panxi region, Southwest China, vanadium titanomagnetite is a kind of widely distributed natural magnetite, in which the iron cations are simultaneously substituted by V^{3+} and Ti^{4+} [11,12]. Vanadium doped magnetite and titanomagnetite have been respectively investigated in previous studies [13,14]. However, until now few systemic studies have been conducted on the magnetite with vanadium and titanium co-doping in the spinel structure. Our recent study has demonstrated that vanadium titanomagnetite showed excellent ability to degrade Acid Orange II through heterogeneous Fenton reaction [15]. But the individual contribution and mechanism of these two substituting cations have not been determined. In addition, photo-Fenton reaction has shown higher efficiency in degradation of organic contaminants than Fenton reaction [16], but so far magnetite used as catalyst in heterogeneous photo-Fenton reaction has been seldom reported.

The main purpose of this study is to elucidate the individual effect of titanium and vanadium on the adsorption and catalytic activity of V-Ti co-doped magnetite in heterogeneous Fenton reaction. UV irradiation near visible light (365 nm) was used in catalytic degradation reaction, which represented a significant advantage for future application in solar photo degradation process [17]. Methylene blue (MB) was selected as a model contaminant since it is non-biodegradable, extensively used in textile industry and usually chosen as a model contaminant in the relative studies. The new insights obtained in this study are of high importance for well understanding the interface interaction between contaminants and natural minerals, and application of natural magnetite in pollution controlling and environmental remediation.

2. Experimental

2.1. Preparation of magnetite samples

All chemicals and reagents used in this study were of analytical grade. Predetermined amount of $FeSO_4$ and $TiCl_4$ was dissolved in an HCl solution. 1.0 mL hydrazine was added to prevent the oxidation of ferrous cations, and pH was low enough (<1) to prevent iron oxidation and hydroxide precipitation. This solution was heated to 90–100 °C under N_2. Equal volume of solution containing 4.0 mol L^{-1} NaOH, 0.90 mol L^{-1} $NaNO_3$ and suitable amount of NH_4VO_3 was added dropwise (10 mL min^{-1}) into the heated iron and titanium solution. The reaction was maintained at 90 °C for 2 h, while mechanical stirring at a rate of 500 rpm. Then the resulted solution was cooled to room temperature. It was necessary to emphasize that, during the reaction, N_2 should be passed through to prevent the oxidation of ferrous cation. In the final solution, the total metal cation concentrations of Fe, V and Ti was 0.45 mol L^{-1}. The particles were then separated by centrifugation at 3500 rpm for 5 min and washed with boiling distilled water, followed by an additional centrifugation. After 3–4 washings, the particles were collected and freeze dried at −50 °C in vacuum for 12 h. Ti doped magnetite as reference sample was synthesized according to the above procedure without adding NH_4VO_3 and V doped magnetite as reference sample was synthesized without adding $TiCl_4$. And Fe_3O_4 also as reference sample was prepared without adding these two chemicals [18,19]. All the magnetite samples were ground and passed through a 200 mesh screen.

2.2. Characterization methods

Total Fe, V and Ti contents in the prepared samples were measured spectrophotometrically with phenanthroline, tungstovanadophosphoric acid and diantipyrylmethane method, respectively.

PXRD patterns were recorded between 10° and 80° (2θ) at a step of 1° min^{-1} on a Bruker D8 advance diffractometer with Cu Kα radiation (40 kV and 40 mA). BET specific surface area was measured on the basis of the N_2 physisorption capacity at 77 K on an ASAP 2020 instrument, after degassed at 433 K for 12 h. Transmission electron microscope (TEM) observation was performed on a JEOL JEM-100CXII instrument at an accelerating voltage of 100 kV. TG analysis was conducted on a Netzsch STA 409 PC instrument at a heating rate of 10 °C min^{-1} under N_2 atmosphere (60 cm^3 min^{-1} at normal temperature and pressure).

The Ti and V K-edge X-ray absorption near edge structure (XANES) spectra of the magnetite samples and reference compounds were collected on the new Wiggler beamline BL14W1of Shanghai Synchrotron Radiation Facility (SSRF).

2.3. Adsorption test

Batch adsorption studies of MB on synthetic magnetite samples were carried out in conical flasks. The temperature was controlled at 25 °C. The initial pH of solution was adjusted to 7.0 by H_2SO_4 and NaOH solution. The suspension containing 20.0 mg dry adsorbent and 20 mL varying concentrations (12.5–100 mg L^{-1}) of MB solution was constantly magnetically stirred for 1 h, predetermined time for achieving adsorption equilibrium. Then the adsorbent was separated by centrifugation and the equilibrium concentration of MB was determined by UV–vis spectrophotometer UV-7504 at a wavelength of 665 nm, the maximum absorption wavelength of MB.

2.4. Catalytic heterogeneous UV-Fenton reaction test

The heterogeneous UV-Fenton degramemade photo-reactor [20] under UV illumination at 25 °C. The dosage of catalyst was 1.0 g L^{-1} while the initial concentrations of MB and H_2O_2 were 0.2 and 10 mmol L^{-1}, respectively. The volume of MB solution was 500 mL. All the experiments were carried out under constant stirring to make the catalyst well dispersed. The initial pH of the system was adjusted to 7.0 by H_2SO_4 and NaOH solution to conduct a heterogeneous system. Before adding H_2O_2, the suspension containing catalyst and MB was stirred for 1 h in the dark to achieve adsorption equilibrium. Then the degradation reaction was initiated by turning on UV light (6 W, 365 nm) and adding H_2O_2 to the system simultaneously. At given intervals of degradation, 5 mL of reaction solution was sampled from the photo-reactor. Immediately the solid catalyst was separated by centrifugation at 3500 rpm for 1 min. The supernatant was sampled and diluted for UV–vis analysis on UV-7504. The UV–vis absorption spectra were measured by PerkinElmer Lamboda 850. The pH of reaction system was monitored by a PHS-3C pH meter (Rex Instrument Factory, Shanghai, China). The concentrations of leaching Fe, V and Ti ions after degradation were determined on an inductively coupled plasma atomic emission spectroscopy (ICP-AES, Varian Vista, America) with the wavelength range of 167–785 nm and the limit detection of 0.01 μg L^{-1}.

3. Results and discussion

3.1. Characterization of magnetite samples

Based on the chemical analysis results, the synthetic magnetite samples were labeled as Fe_3O_4, $Fe_{2.31}Ti_{0.69}O_4$, $Fe_{2.43}Ti_{0.54}V_{0.03}O_4$, $Fe_{2.50}Ti_{0.42}V_{0.08}O_4$, $Fe_{2.47}Ti_{0.40}V_{0.13}O_4$ and $Fe_{2.68}V_{0.32}O_4$, respectively. Among the doped magnetite samples, the titanium content gradually decreases while that of vanadium accordingly increases, but iron content shows less variation.

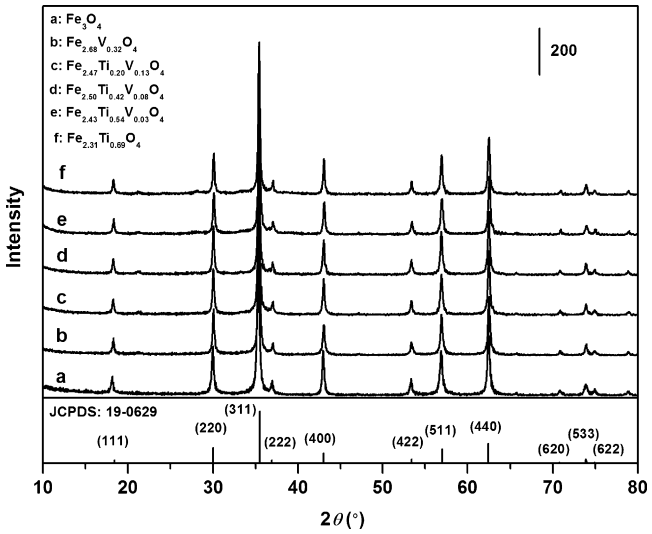

Fig. 1. PXRD patterns for all the synthetic magnetite samples.

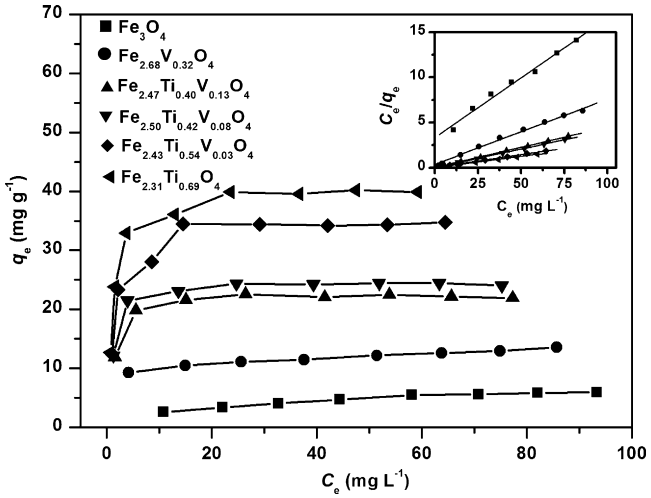

Fig. 3. Adsorption isotherms of MB on synthetic magnetite samples (C_0 = 12.5–100 mg L^{-1}, 1.0 g L^{-1} of magnetite sample, 20 mL, pH 7.0, 25 °C). Inset: adsorption isotherms fitted by Langmuir model.

Fig. 1 shows the PXRD patterns of all the magnetite samples. The characteristic reflections of all the samples well correspond to the standard card of magnetite (JCPDS: 19-0629), indicating that the synthetic samples have well crystallized spinel structure and the introduction of vanadium and titanium shows no obvious effect on the crystal structure of magnetite. From their TEM images (Fig. 2), most of the particles are less than 100 nm in size and grow well in an octahedral shape, which is the typical morphology of well crystallized magnetite. A test with the magnet showed that all the prepared samples are magnetic and completely attracted to the magnet, which is helpful for their practical application in wastewater decontamination with facile recycle.

3.2. Adsorption and catalytic activity of magnetite samples

Fig. 3 shows the adsorption isotherms of MB on different magnetite samples at neutral pH. These adsorption isotherms are well fitted by the Langmuir model [21] with the corrective coefficient R^2 ranging in 0.991-0.999. The saturated adsorbed amount and the adsorption equilibrium constant are shown in Table 1. The saturated adsorbed amount of all the doped magnetite samples is greater than that of Fe_3O_4, indicating that the introduction of Ti and V can enhance the adsorption activity of magnetite. Moreover, for V-Ti co-doped magnetite samples, the saturated adsorbed amount strongly depends on the Ti content rather than that of V, suggesting that Ti has more positive effect on the adsorption activity of magnetite than V does.

Fig. 4 shows the MB decolorization under various conditions. Without any solid catalyst, MB was slowly decolorized by H_2O_2 and UV, demonstrating that MB could be tardily degraded by H_2O_2 under UV. The mechanism of this process is the photolysis of H_2O_2 into hydroxyl radicals •OH (Eq. (1)) [22]. •OH radical has a quite high redox potential and can oxidize most organic molecules.

$$H_2O_2 + h\nu \rightarrow 2^{\bullet}OH \quad (1)$$

In the dark with the presence of H_2O_2 and catalyst $Fe_{2.43}Ti_{0.54}V_{0.03}O_4$, the process displayed an efficient degradation rate through the heterogeneous Fenton reaction [5,9], where Fe^{2+} and doping cations on magnetite surface could activate H_2O_2 in a Haber–Weiss mechanism to produce the •OH radical.

With the introduction of UV illumination and H_2O_2, the degradation catalyzed by $Fe_{2.43}Ti_{0.54}V_{0.03}O_4$ was greatly improved, due

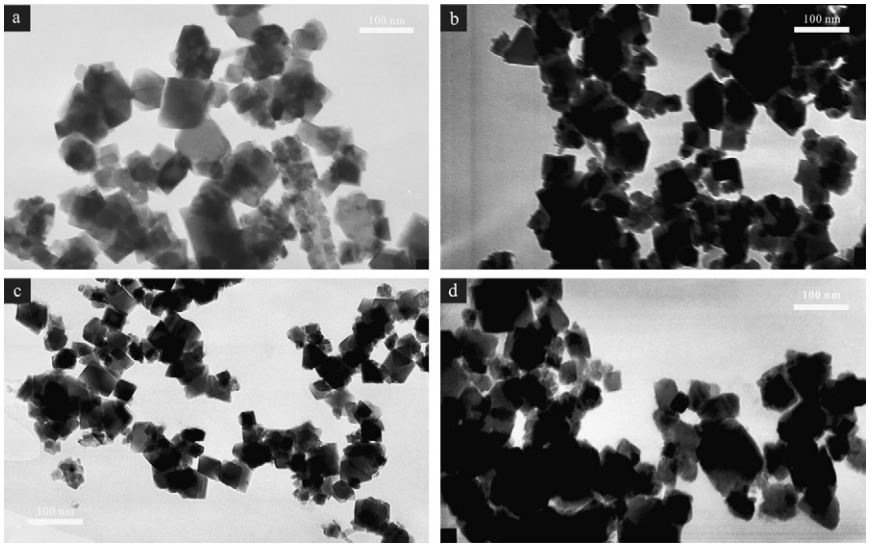

Fig. 2. TEM images of some synthetic magnetite samples (a: Fe_3O_4; b: $Fe_{2.68}V_{0.32}O_4$; C: $Fe_{2.50}Ti_{0.42}V_{0.08}O_4$; d: $Fe_{2.31}Ti_{0.69}O_4$).

Table 1
The saturated adsorbed amount, Langmuir isotherm constants and adsorption equations for MB adsorbed on magnetite samples.

Sample	Q_{max}[a] (mg g^{-1})	Adsorption equations	K_a	R^2
Fe_3O_4	7.57	$C_e/q_e = 3.315 + 0.132C_e$	0.04	0.991
$Fe_{2.68}V_{0.32}O_4$	13.9	$C_e/q_e = 0.381 + 0.072C_e$	5.29	0.993
$Fe_{2.47}Ti_{0.40}V_{0.13}O_4$	22.7	$C_e/q_e = 0.026 + 0.044C_e$	0.59	0.999
$Fe_{2.50}Ti_{0.42}V_{0.08}O_4$	25.0	$C_e/q_e = 0.027 + 0.040C_e$	0.68	0.999
$Fe_{2.43}Ti_{0.54}V_{0.03}O_4$	35.7	$C_e/q_e = 0.039 + 0.028C_e$	1.39	0.999
$Fe_{2.31}Ti_{0.69}O_4$	41.7	$C_e/q_e = 0.029 + 0.024C_e$	1.21	0.999

[a] Q_{max}: saturated adsorbed amount.

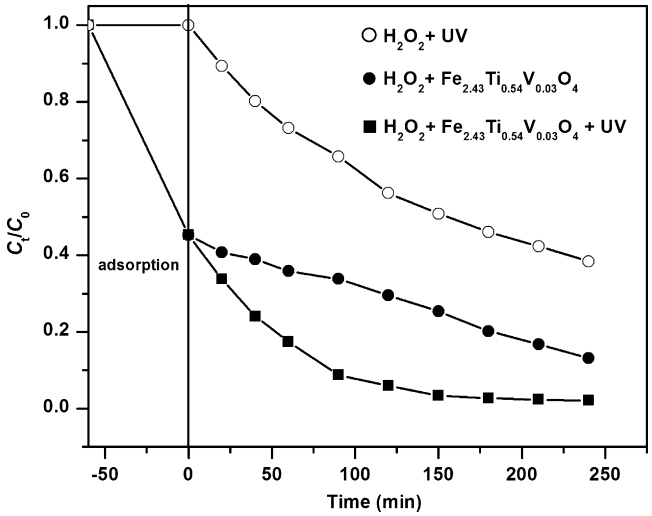

Fig. 4. MB degradation under various conditions.

to the fact that Fe^{3+} reduction could occur in the presence of UV light and result in the generation of Fe^{2+}, whose catalytic activity was much stronger than that of Fe^{3+} (Eqs. (2) and (3)) [16,23].

$$\equiv Fe_{surf}{}^{2+} + H_2O_2 \rightarrow \equiv Fe_{surf}{}^{3+} + {}^{\bullet}OH + HO^- \quad (2)$$

$$\equiv Fe_{surf}{}^{3+} + HO^- + h\nu \rightarrow \equiv Fe_{surf}{}^{2+} + {}^{\bullet}OH \quad (3)$$

Prior to the H_2O_2 introduction and UV illumination, the decolorization of MB only relied on the adsorption by magnetite catalysts (Figs. 4 and 5). In Fig. 5, the decolorization rate by adsorption increased with the increase of Ti content in samples, due to the increase of adsorption activity. After adding H_2O_2 and introducing UV illumination simultaneously, the decolorization was greatly accelerated. After 120 min, about 96%, 94%, 85%, 83%, 70%, 61% and 48% of MB was decolorized by $Fe_{2.31}Ti_{0.69}O_4$, $Fe_{2.43}Ti_{0.54}V_{0.03}O_4$, $Fe_{2.50}Ti_{0.42}V_{0.08}O_4$, $Fe_{2.47}Ti_{0.40}V_{0.13}O_4$, $Fe_{2.68}V_{0.32}O_4$ and Fe_3O_4, respectively. After 240 min, the decolorization efficiencies for the systems catalyzed by $Fe_{2.31}Ti0_{.69}O_4$, $Fe_{2.43}Ti_{0.54}V_{0.03}O_4$, $Fe_{2.50}Ti_{0.42}V_{0.08}O_4$ and $Fe_{2.47}Ti_{0.40}V_{0.13}O_4$, respectively, were above 90%. As reported by previous studies [24,25], the kinetic study of UV-Fenton process can be performed by assuming that the reaction between hydroxyl radicals and the pollutant is the rate determining step. Thus, by assuming that •OH instantaneous concentration was a constant, MB degradation could be described by a pseudo-first-order kinetic expression:

$$-\frac{dC}{dt} = k \times C_{\bullet OH} \times C = k_{app} \times C \rightarrow -\ln\frac{C_0}{C} = k_{app} \times t \quad (4)$$

where C is the MB concentration, mg L^{-1}, k is the reaction rate constant and k_{app} is the apparent pseudo-first-order constant. The insert figure in Fig. 5 shows the results of Fig. 5 plotted in the form of Eq. (4). Straight lines passing through the origin fit the degradation data well (the coefficient of linear regression, r, is all greater than 0.99) and from the slopes, k_{app} values were 0.0181, 0.0162, 0.010, 0.0093, 0.0054, 0.0044 and 0.0034 min^{-1} for the systems catalyzed by $Fe_{2.31}Ti0_{.69}O_4$, $Fe_{2.43}Ti_{0.54}V_{0.03}O_4$, $Fe_{2.50}Ti_{0.42}V_{0.08}O_4$, $Fe_{2.47}Ti_{0.40}V_{0.13}O_4$, $Fe_{2.68}V_{0.32}O_4$, Fe_3O_4 and no solid catalyst, respectively. All k_{app} of the systems with magnetite/H_2O_2/UV were higher than that of the system with only H_2O_2/UV, indicating that magnetite could improve the degradation efficiency of heterogeneous UV-Fenton reaction. Also the incorporation of V and Ti could improve the catalytic activity of magnetite, but obviously the degradation rate strongly depended on the content of Ti rather than that of V. That is to say, magnetite with high content of Ti (accordingly with low V content) shows higher degradation rate than that with high content of V (accordingly with low Ti content).

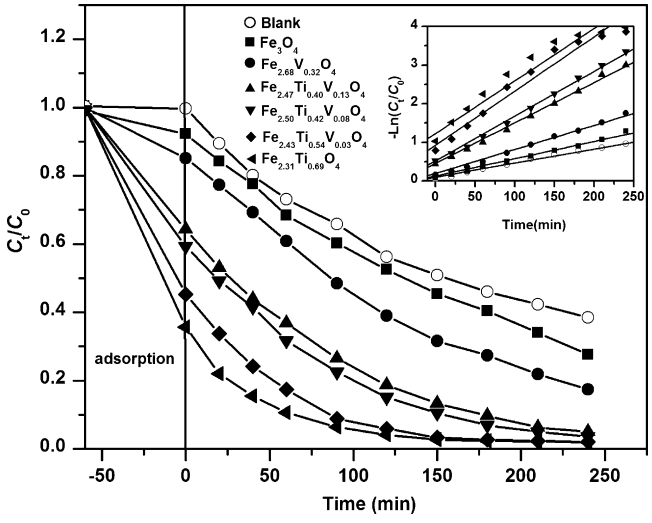

Fig. 5. UV-Fenton degradation of MB catalyzed by synthetic magnetite samples (C_0 = 0.2 mmol L^{-1}, 10 mmol L^{-1} of H_2O_2, 1.0 g L^{-1} of catalyst, UV (6 W, 365 nm), 500 mL, pH 7.0, 25 °C). Inset: UV-Fenton degradation processes fitted by pseudo-first-order kinetics.

To investigate to the transformation of degradation products, UV–vis inspection of the degradation process catalyzed by $Fe_{2.43}Ti_{0.54}V_{0.03}O_4$ was carried out (Fig. 6). In the initial adsorption step, the original UV–vis absorption spectrum of MB mainly consisted of four peaks at 246, 292, 602 and 665 nm [26]. During the UV-Fenton degradation, intensities of the absorption peaks at 200, 246, 292, 602 and 665 nm decreased with the increase of reaction time. Obviously, the decrease of the peak intensity at 200 nm corresponded to H_2O_2 decomposition. And the decrease of the other peak intensities was ascribed to MB degradation. A quick decrease of the absorption bands at 665 and 602 nm was ascribed to the N-demethylation of MB. The bands at 246 and 292 nm decreased significantly and no new bands appeared. This implies that a full oxidative decomposition of the phenothiazine species has occurred and no intermediates containing the phenothiazine moiety was formed [26]. Therefore, N-demethylation, deamination and oxidative degradation have taken place during MB degradation.

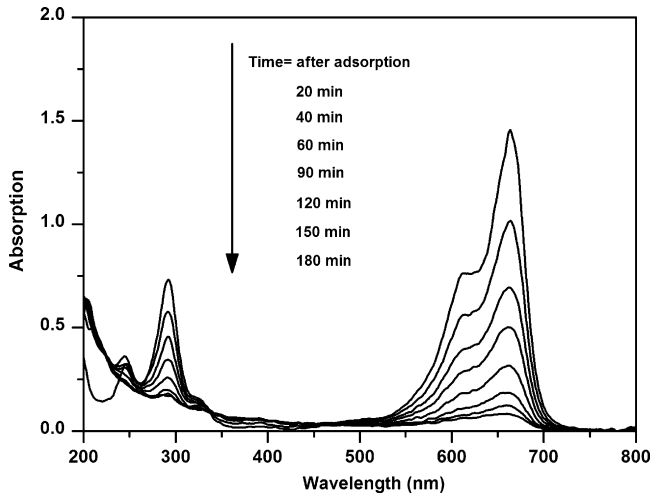

Fig. 6. The changes of MB absorption spectra with the reaction time during the UV-Fenton reaction (C_0 = 0.2 mmol L^{-1}, 10 mmol L^{-1} of H_2O_2, 1.0 g L^{-1} of $Fe_{2.43}Ti_{0.54}V_{0.03}O_4$, UV (6 W, 365 nm), 500 mL, pH 7.0, 25 °C).

After degradation, the pH of all the degradation systems was in the range of 5.0–6.0 and the decrease of pH value was due to the appearance of several intermediate acidic products [27]. From previous research [28], when the pH of degradation system is above 4.0, the amount of dissolved iron ion is so low that the effect of homogeneous reaction on the degradation process can be neglected. In this study, the final pH value of all the system was above 5.0 and the final concentration of dissolved iron ion in all the degradation systems was below 0.03 mg L^{-1}, indicating that the homogeneous reaction catalyzed by dissolved iron can be neglected. Moreover, for both dissolved titanium and vanadium ions, their final concentrations in all the systems were no more than 0.01 mg L^{-1}, illustrating that the contribution of homogeneous reaction catalyzed by the leaching of V or Ti ions can also be neglected. Therefore, the decomposition of MB was mainly ascribed to heterogeneous photo-Fenton reaction.

3.3. Mechanism of V-Ti substitution improving adsorption and catalytic activity

In this study, magnetite sample containing more Ti and less V shows better adsorption and catalytic activity, though both Ti and V can improve the activity of magnetite. MB adsorption is closely related to the surface properties of the used adsorbent, including specific surface area, point of zero charge (PZC) and the amount of superficial hydroxyl [29–31]. The catalytic activity of metal-substituted magnetite is mainly associated with the valence and occupancy of the doping metals [10]. Herein, complementary characterization technologies were utilized to investigate the influence of substituted cations on the above-mentioned properties, which is of high importance for well understanding the contribution and mechanism of V and Ti substitution on improving the adsorption and catalytic activity of magnetite.

3.3.1. Valence and occupancy of doping metals

XANES measurement was carried out to probe the coordination environment of V and Ti cations, which is closely related to the catalytic activity of magnetite. Fig. 7 shows the normalized Ti K-edge XANES spectra of synthetic magnetite samples and Ti reference compounds. For Ti foil, its absorption edge which is defined as the maximum of derivative at the absorption edge locates at 4965.0 eV. For rutile (α-TiO_2), its absorption edge locates at 4981.4 eV with a pre-edge peak at 4971.7 eV [32], while the XANES spectrum of anatase (γ-TiO_2) shows an absorption edge at 4978.9 eV with a more obvious pre-edge peak at 4970.5 eV and a shoulder peak at

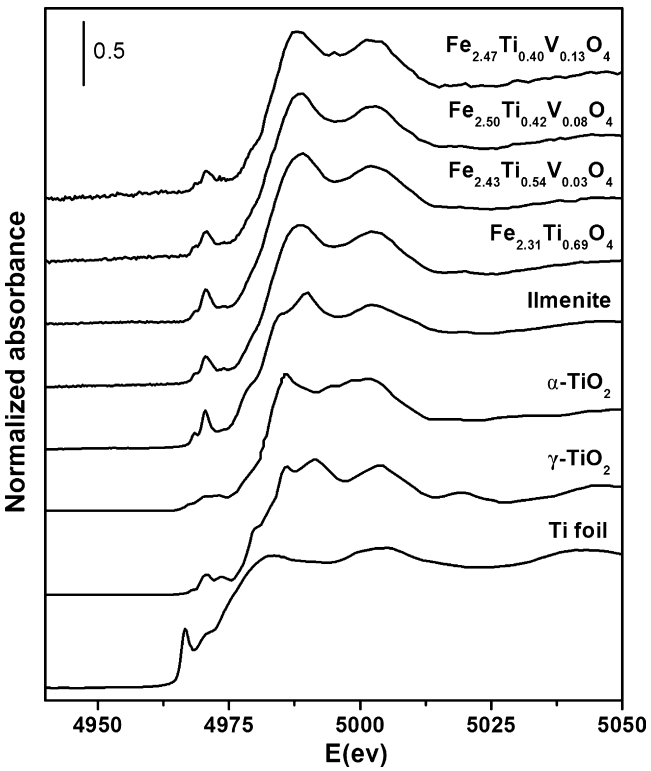

Fig. 7. The Ti K-edge XANES spectra for synthetic magnetite samples and Ti reference compounds.

4979.5 eV [33]. For ilmenite ($FeTiO_3$), the XANES spectrum shows an absorption edge at 4980.4 eV with a strong pre-edge peak at 4970.4 eV and two shoulder peaks at 4979.4 and 4984.8 eV. The Ti K-edge XANES spectra of Ti doped samples do not show obvious variations. The absorption K-edge is at 4981.0 eV with a weak pre-edge peak at 4970.7 eV and a shoulder peak at 4979.4 eV. The energy position of Ti absorption peak of magnetite samples is quite close to that of rutile, anatase and ilmenite where Ti cations are in the valence of +4, but far from that of Ti foil. Therefore, the valence of Ti cations in the magnetite samples should be +4. From Fig. 7, it can be seen that all the XANES spectra of Ti-doped magnetite samples are completely different from those of the reference compounds, indicating that Ti cations in magnetite are impossible to exist as secondary phase like the reference compounds, and should be doped in the spinel structure. This conclusion is in accordance with that obtained from XRD characterization. Generally, the pre-edge peak related to tetrahedral site should be stronger than that of octahedral one, due to the low symmetry of tetrahedral site. In the present study, the pre-edge peak of Ti in magnetite is quite weak, implying that Ti^{4+} mainly occupied the octahedral sites rather than tetrahedral ones.

The normalized V K-edge XANES spectra for V doped magnetite samples and V reference compounds are shown in Fig. 8. For V foil, its absorption peak is at 5465.0 eV with no pre-edge peak. For V_2O_3, the V K-edge XANES shows a absorption edge at 5480.5 eV, with a very weak pre-edge peak at 5469.1 eV. On the K-edge XANES spectrum of VO_2, the absorption edge is located at 5483.2 eV and a pre-edge peak is observed at 5470.3 eV with a larger intensity than that of V_2O_3. For V_2O_5, a very sharp pre-edge appears at 5469.9 eV and the absorption edge is at 5484.3 eV. The XANES spectra of V doped magnetite samples display a feather rather different from those of vanadium oxides. For sample $Fe_{2.47}Ti_{0.54}V_{0.03}O_4$, a weak pre-edge peak appears at 5468.8 eV and the absorption edge shows a strong peak at 5478.6 eV with two obvious shoulder peaks at

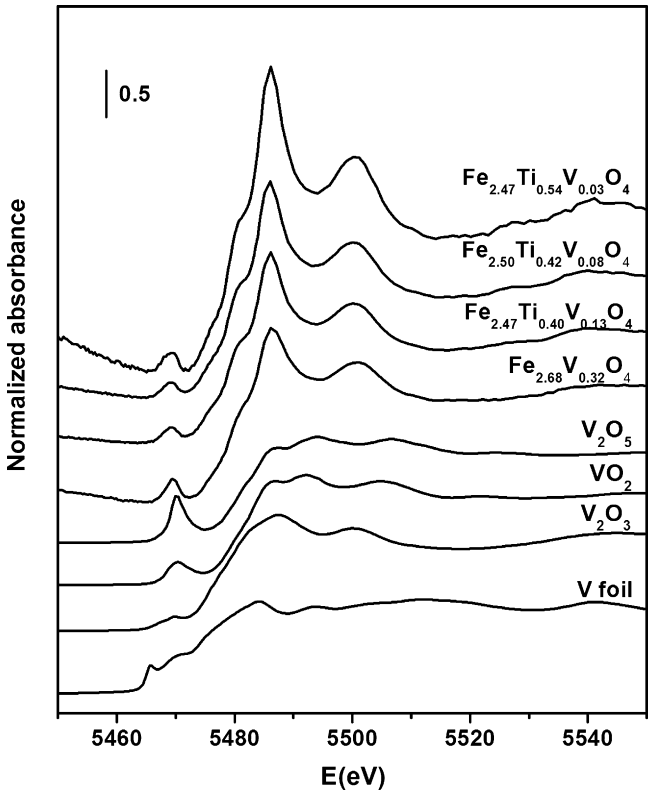

Fig. 8. The V K-edge XANES spectra for synthetic magnetite samples and V reference compounds.

5474.6 and 5480.0 eV. The energy position of the absorption peak is similar to that of V_2O_3. This indicates that vanadium in this magnetite sample exists as V^{3+}. With the increase of vanadium content, the XANES spectra of V doped magnetite samples do not show any obvious variation, suggesting that the valence and the coordination of vanadium in the magnetite samples are similar. Their XANES spectra are completely different from those of the reference compounds, indicating that these V cations are impossible to exist as secondary phase like V metal, V_2O_3, VO_2 or V_2O_5, and should be incorporated into the spinel structure. The low pre-edge peak indicates V^{3+} mainly occupied the octahedral sites.

Here, it can be found that both of Ti and V occupy the octahedral sites of magnetite in valence of +4 and +3, respectively. The valence and occupancy of the two doping metals in co-doped magnetite are similar to the case of single-metal-substitution magnetites and natural magnetite [34].

3.3.2. BET special surface area

Table 2 shows the lattice parameter a_0, crystal size, specific surface area and pore volume of all the prepared samples. It can be seen that the introduction of V and Ti cations does not obviously change the lattice parameter a_0, due to the close value of cationic radii for Ti^{4+} (68 pm), V^{3+} (64 pm) and replaced Fe^{3+} (65 pm) in the octahedral site [14,35]. Also, the crystal size and pore volume are quite close to those of synthetic Fe_3O_4. However, the specific surface area obviously increases with the increment of titanium content, and $Fe_{2.31}Ti_{0.69}O_4$ sample with the highest titanium content in all synthetic magnetites shows the largest specific surface area. Contrarily, the specific surface area of $Fe_{2.68}V_{0.32}O_4$ with the highest vanadium content is quite close to that of Fe_3O_4. This suggests that the incorporation of titanium has an obvious effect on increasing the specific surface area of magnetite.

3.3.3. Superficial hydroxyl

The dehydroxylation of magnetite occurs in the range of 150–400 °C [36]. In this study, TG analysis under N_2 was used to investigate the amount of superficial hydroxyl in the prepared samples. The mass losses related to dehydroxylation for Fe_3O_4, $Fe_{2.68}V_{0.32}O_4$, $Fe_{2.47}Ti_{0.40}V_{0.13}O_4$, $Fe_{2.50}Ti_{0.42}V_{0.08}O_4$, $Fe_{2.43}Ti_{0.54}V_{0.03}O_4$ and $Fe_{2.31}Ti0_{.69}O_4$ are 1.21%, 1.23%, 1.23%, 1.28%, 1.57% and 1.60%, respectively, illustrating that titanium substitution has a more significant effect on the amount of superficial hydroxyl than vanadium does. From previous studies, superficial hydroxyl group is mainly derived from the dissociation of water molecules adsorbed on the oxygen defect [37,38]. On the V-Ti co-doped magnetite surface, the superficial hydroxyl groups include Fe-OH, Ti-OH and V-OH. XANES characterization has demonstrated that both Ti^{4+} and V^{3+} have incorporated into the spinel structure by replacing Fe^{3+}. Obviously, isomorphic substitution of Fe^{3+} by Ti^{4+} would result in positively charged surface in magnetite and these net positive surface charges will be balanced by superficial hydroxyls via dissociation of adsorbed water molecules.

3.3.4. Mechanism of metal substitution on increasing adsorption and catalytic activity

The introduction of Ti and V obviously improved the adsorption activity of magnetite, and the saturated adsorbed amount of MB on magnetite obviously depends on the Ti content rather than V. On the basis of the obtained characterization results, there are two possible explanations for this phenomenon. One is that the prominent increase of specific surface area with the increment of Ti incorporation provides more surface area for the coverage of MB. And the other one corresponds to the increase of superficial hydroxyl amount on magnetite surface. TG analysis under N_2 shows that the superficial hydroxyl amount increases with the increment of Ti content. From the previous researches, the main mechanism of MB adsorption on the magnetite is the columbic or electrostatic interaction between MB and magnetite surface [29,39]. As MB is a cationic dye and the pH_{zpc} of the magnetite samples is lower than 7.0 (Table 2), when the solution pH is above pH_{zpc}, the magnetite surface is negatively charged and the net negative surface charges increase with the increment of superficial hydroxyl amount, resulting in more MB cations adsorbed on the magnetite surface (Eqs. (5) and (6)).

$$\text{M-OH} + {}^{-}\text{OH} \leftrightarrow \text{M-O}^{-} + \text{H}_2\text{O} \quad (5)$$

$$\text{M-O}^{-} + {}^{+}\text{MB} \leftrightarrow \text{M-O}^{-+}\text{MB} \quad (6)$$

Table 2
Lattice parameter a_0, crystal size, specific surface area, pore volume and PZC for all the synthetic magnetite samples.

Sample	Lattice parameter, a_0 (nm)	Crystal size (nm)	Specific surface area ($m^2\ g^{-1}$)	Pore volume ($cm^3\ g^{-1}$)	PZC[a]
Fe_3O_4	0.8411	28.2	27.84	0.219	6.92
$Fe_{2.68}V_{0.32}O_4$	0.8390	31.5	27.33	0.206	6.14
$Fe_{2.47}Ti_{0.40}V_{0.13}O_4$	0.8397	29.5	40.79	0.237	6.15
$Fe_{2.50}Ti_{0.42}V_{0.08}O_4$	0.8390	30.6	39.58	0.216	6.09
$Fe_{2.43}Ti_{0.54}V_{0.03}O_4$	0.8383	28.1	47.26	0.305	6.89
$Fe_{2.31}Ti_{0.69}O_4$	0.8390	31.3	50.74	0.268	6.67

[a] PZC: point of zero charge.

Our present study has demonstrated that the introduction of Ti^{4+} and V^{3+} can greatly promote the catalytic activity of magnetite in heterogeneous UV-Fenton reaction. In the case of V incorporation, since vanadium has thermodynamically favorable redox pairs (V^{2+}/V^{3+} and V^{3+}/V^{4+}), V^{3+} on the magnetite surface can decompose H_2O_2 to produce OH and improve the electron transfer to produce Fe^{2+} during the reaction [40,41], resulting in an improvement of catalytic activity of magnetite. For the incorporation of Ti, although Ti does not have a thermodynamically favorable redox pair, Ti^{4+} can effectively create the hole-electron pair under UV-light and produce •OH for MB degradation [42,43]. Moreover, Ti^{4+} has a more significant effect on the increase of specific surface area and superficial hydroxyl amount than V does, which can greatly improve the adsorption activity of the obtained magnetite and accordingly accelerate the degradation of MB [44].

4. Conclusions

Our present study has shown that both vanadium and titanium have been introduced into the synthetic magnetite with well crystallized spinel structure, where both vanadium in valence of +3 and titanium in valence of +4 occupy the octahedral sites. The incorporation of Ti^{4+} and V^{3+} can greatly enhance UV-Fenton catalytic activity of magnetite during the MB decolorizaiton through two different ways. The V incorporation will accelerate the decomposition of H_2O_2 to produce OH via favorable redox pairs (V^{2+}/V^{3+} and V^{3+}/V^{4+}), resulting in an improvement of catalytic activity of magnetite. In the other hand, the incorporation of Ti results in a significant increase of specific surface area and superficial hydroxyl amount, and accordingly improves the adsorption activity of magnetite to MB. The improvement of the adsorption activity of magnetite to MB will lead to the acceleration of MB degradation. Also, Ti^{4+} shows a more prominent effect than V^{3+} on improving the adsorption and catalytic activity of magnetite. The obtained novel insights are of high importance for well understanding the interface interaction between contaminants and metal doped magnetites, and the environmental application of natural and synthetic magnetites.

Acknowledgement

This is contribution No. IS-1406 from GIG CAS. We would like to thank Shanghai Synchrotron Radiation Facility (SSRF) for providing us the beam time for the XANES measurement. This work is financially supported by National Natural Science Foundation of China (Grant Nos. 40773060 and 41172045).

References

[1] V.S. Coker, C.I. Pearce, R.A.D. Pattrick, G. Van der Laan, N.D. Telling, J.M. Charnock, E. Arenholz, J.R. Lloyd, Probing the site occupancies of Co-, Ni-, and Mn-substituted biogenic magnetite using XAS and XMCD, Am. Mineral. 93 (2008) 1119–1132.
[2] T.L. Jentzsch, C.L. Chun, R.S. Gabor, R.L. Penn, Influence of aluminum substitution on the reactivity of magnetite nanoparticles, J. Phys. Chem. C 111 (2007) 10247–10253.
[3] C.R. De Silva, S. Smith, I. Shim, J. Pyun, T. Gutu, J. Jiao, Z.P. Zheng, Lanthanide(III)-doped magnetite nanoparticles, J. Am. Chem. Soc. 131 (2009) 6336–6337.
[4] P. Baldrian, V. Merhautova, J. Gabriel, F. Nerud, P. Stopka, M. Hruby, M.J. Benes, Decolorization of synthetic dyes by hydrogen peroxide with heterogeneous catalysis by mixed iron oxides, Appl. Catal. B: Environ. 66 (2006) 258–264.
[5] R.C.C. Costa, M.F.F. Lelis, L.C.A. Oliveira, J.D. Fabris, J.D. Ardisson, R.R.V.A. Rios, C.N. Silva, R.M. Lago, Novel active heterogeneous Fenton system based on $Fe_{3-x}M_xO_4$ (Fe, Co, Mn, Ni): The role of M^{2+} species on the reactivity towards H_2O_2 reactions, J. Hazard. Mater. 129 (2006) 171–178.
[6] R.C.C. Costa, M. de Fatima, F. Lelis, L.C.A. Oliveira, J.D. Fabris, J.D. Ardisson, R.R.V.A. Rios, C.N. Silva, R.M. Lago, Remarkable effect of Co and Mn on the activity of $Fe_{3-x}M_xO_4$ promoted oxidation of organic contaminants in aqueous medium with H_2O_2, Catal. Commun. 4 (2003) 525–529.
[7] J. Liu, C.I. Pearce, O. Qafoku, E. Arenholz, S. Heald, T. Peretyazhko, K.M. Rosso, Reduction of contaminant Tc(VII) by magnetite (Fe_3O_4) and titanomagnetite ($Fe_{3-x}Ti_xO_4$) nanoparticles, Geochim. Cosmochim. Acta 74 (2010) A615.
[8] A.C.S. da Costa, I.G. Souza, M.A. Batista, K.L. da Silva, J.V. Bellini, A. Paesano, Structural, magnetic and hyperfine characterization of zinc-substituted magnetites, Hyperfine Interact. 175 (2007) 103–111.
[9] F. Magalhaes, M.C. Pereira, S.E.C. Botrel, J.D. Fabris, W.A. Macedo, R. Mendonca, R.M. Lago, L.C.A. Oliveira, Cr-containing magnetites $Fe_{3-x}Cr_xO_4$: The role of Cr^{3+} and Fe^{2+} on the stability and reactivity towards H_2O_2 reactions, Appl. Catal. A: Gen. 332 (2007) 115–123.
[10] C.G. Ramankutty, S. Sugunan, Surface properties and catalytic activity of ferrospinels of nickel, cobalt and copper, prepared by soft chemical methods, Appl. Catal. A: Gen. 218 (2001) 39–51.
[11] M.F. Zhou, C.Y. Wang, K.N. Pang, G.J. Shellnutt, Y. Ma, Origin of giant Fe-Ti-V oxide deposits in layered gabbroic intrusions, Pan-Xi district, Sichuan province, SW China, Mineral Deposit Research: Meeting the Global Challenge, vols. 1 and 2, 2005, pp. 511–513.
[12] X.F. Lei, X.X. Xue, Preparation of perovskite type titanium-bearing blast furnace slag photocatalyst doped with sulphate and investigation on reduction Cr(VI) using UV–vis light, Mater. Chem. Phys. 112 (2008) 928–933.
[13] S.J. Yang, H.P. He, D.Q. Wu, D. Chen, X.L. Liang, Z.H. Qin, M.D. Fan, J.X. Zhu, P. Yuan, Decolorization of methylene blue by heterogeneous Fenton reaction using $Fe_{3-x}Ti_xO_4$ ($0 \le x \le 0.78$) at neutral pH values, Appl. Catal. B: Environ. 89 (2009) 527–535.
[14] I.L. Junior, J.M.M. Millet, M. Aouine, M. do Carmo Rangel, The role of vanadium on the properties of iron based catalysts for the water gas shift reaction, Appl. Catal. A: Gen. 283 (2005) 91–98.
[15] X.L. Liang, Y.H. Zhong, S.Y. Zhu, J.X. Zhu, P. Yuan, H.P. He, J. Zhang, The decolorization of Acid Orange II in non-homogeneous Fenton reaction catalyzed by natural vanadium-titanium magnetite, J. Hazard. Mater. 181 (2010) 112–120.
[16] H. Kusic, N. Koprivanac, L. Srsan, Azo dye degradation using Fenton type processes assisted by UV irradiation: a kinetic study, J. Photochem. Photobiol. A 181 (2006) 195–202.
[17] C.P. Huang, Y.H. Huang, Application of an active immobilized iron oxide with catalytic H_2O_2 for the mineralization of phenol in a batch photo-fluidized bed reactor, Appl. Catal. A: Gen. 357 (2009) 135–141.
[18] W. Yu, T.L. Zhang, H. Zhang, X.J. Qiao, L. Yang, Y.H. Liu, The synthesis of octahedral nanoparticles of magnetite, Mater. Lett. 60 (2006) 2998–3001.
[19] S. Pirillo, M.L. Ferreira, E.H. Rueda, Adsorption of alizarin, eriochrome blue black R, and fluorescein using different iron oxides as adsorbents, Ind. Eng. Chem. Res. 46 (2007) 8255–8263.
[20] J.X. Chen, L.Z. Zhu, Catalytic degradation of Orange II by UV-Fenton with hydroxyl-Fe-pillared bentonite in water, Chemosphere 65 (2006) 1249–1255.
[21] E.D. van Hullebusch, A. Peerbolte, M.H. Zandvoort, P.N.L. Lens, Sorption of cobalt and nickel on anaerobic granular sludges: isotherms and sequential extraction, Chemosphere 58 (2005) 493–505.
[22] E.S. Elmolla, M. Chaudhuri, Comparison of different advanced oxidation processes for treatment of antibiotic aqueous solution, Desalination 256 (2010) 43–47.
[23] G. Ghiselli, W.F. Jardim, M.I. Litter, H.D. Mansilla, Destruction of EDTA using Fenton and photo-Fenton-like reactions under UV-A irradiation, J. Photochem. Photobiol. A 167 (2004) 59–67.
[24] M.I. Pariente, F. Martinez, J.A. Melero, J.A. Botas, T. Velegraki, N.P. Xekoukoulotakis, D. Mantzavinos, Heterogeneous photo-Fenton oxidation of benzoic acid in water: effect of operating conditions reaction by-products and coupling with biological treatment, Appl. Catal. B: Environ. 85 (2008) 24–32.
[25] I. Oller, S. Malato, J.A. Saanchez-Perez, M.I. Maldonado, W. Gernjak, L.A. Perez-Estrada, J.A. Munoz, C. Ramos, C. Pulgarin, Pre-industrial-scale combined solar photo-Fenton and immobilized Biomass activated-sludge biotreatment, Ind. Eng. Chem. Res. 46 (2007) 7467–7475.
[26] T.Y. Zhang, T. Oyama, A. Aoshima, H. Hidaka, J.C. Zhao, N. Serpone, Photooxidative N-demethylation of methylene blue in aqueous TiO_2 dispersions under UV irradiation, J. Photochem. Photobiol. A 140 (2001) 163–172.
[27] H. Ma, Q. Zhuo, B. Wang, Characteristics of CuO-MoO_3-P_2O_5 catalyst and its catalytic wet oxidation (CWO) of dye wastewater under extremely mild conditions, Environ. Sci. Technol. 41 (2007) 7491–7496.
[28] S.S. Chou, C.P. Huang, Y.H. Huang, Heterogeneous and homogeneous catalytic oxidation by supported gamma-FeOOH in a fluidized bed reactor: kinetic approach, Environ. Sci. Technol. 35 (2001) 1247–1251.
[29] R.C. Wu, J.H. Qu, Removal of azo dye from water by magnetite adsorption-Fenton oxidation, Water Environ. Res. 76 (2004) 2637–2642.
[30] S.B. Wang, Z.H. Zhu, A. Coomes, F. Haghseresht, G.Q. Lu, The physical and surface chemical characteristics of activated carbons and the adsorption of methylene blue from wastewater, J. Colloid Interf. Sci. 284 (2005) 440–446.
[31] V.K. Gupta, S. Agarwal, T.A. Saleh, Chromium removal by combining the magnetic properties of iron oxide with adsorption properties of carbon nanotubes, Water Res. 45 (2011) 2207–2212.
[32] N. Jiang, D. Su, J.C.H. Spence, Determination of ti coordination from pre-edge peaks in Ti K-edge XANES, Phys. Rev. B 76 (2007) 214111–214118, 214117.
[33] Y.C. Nah, I. Paramasivam, P. Schmuki, Doped TiO_2 and TiO_2 nanotubes: synthesis and applications, ChemPhysChem 11 (2010) 2698–2713.
[34] E. Balan, J.P.R. De Villiers, S.G. Eeckhout, P. Glatzel, M.J. Toplis, E. Fritsch, T. Allard, L. Galoisy, G. Calas, The oxidation state of vanadium in titanomagnetite from layered basic intrusions, Am. Miner. 91 (2006) 953–956.

[35] C.A. Barrero, K.E. Garcia, A.L. Morales, J.M. Greneche, Fe-57 Mossbauer study of beta-FeOOH obtained in presence of Al^{3+} and Ti^{4+} ions, Physica B: Condensed Matter. 389 (2007) 88–93.
[36] D. Thickett, M. Odlyha, Application of thermomagnetometry to corrosion studies of archaeological iron, J. Therm. Anal. Calorim. 80 (2005) 565–571.
[37] M. Chiesa, M.C. Paganini, E. Giamello, D.M. Murphy, C. Di Valentin, G. Pacchioni, Excess electrons stabilized on ionic oxide surfaces, Acc. Chem. Res. 39 (2006) 861–867.
[38] A. Calzolari, A. Catellani, Water adsorption on nonpolar ZnO(1 0 1 0) surface: a microscopic understanding, J. Phys. Chem. C 113 (2009) 2896–2902.
[39] M.A. Al-Ghouti, M.A.M. Khraisheh, M.N.M. Ahmad, S. Allen, Adsorption behaviour of methylene blue onto Jordanian diatomite: a kinetic study, J. Hazard. Mater. 165 (2009) 589–598.
[40] X.L. Liang, S.Y. Zhu, Y.H. Zhong, J.X. Zhu, P. Yuan, H.P. He, J. Zhang, The remarkable effect of vanadium doping on the adsorption and catalytic activity of magnetite in the decolorization of methylene blue, Appl. Catal. B: Environ. 97 (2010) 151–159.
[41] J.H. Deng, J.Y. Jiang, Y.Y. Zhang, X.P. Lin, C.M. Du, Y. Xiong, $FeVO_4$ as a highly active heterogeneous Fenton-like catalyst towards the degradation of Orange II, Appl. Catal. B: Environ. 84 (2008) 468–473.
[42] T. Sano, N. Negishi, K. Koike, K. Takeuchi, S. Matsuzawa, Preparation of a visible light-responsive photocatalyst from a complex of Ti^{4+} with a nitrogen-containing ligand, J. Mater. Chem. 14 (2004) 380–384.
[43] M.J. Rosseinsky, J.H. Clark, M.S. Dyer, R.G. Palgrave, C.P. Ireland, J.R. Darwent, J.B. Claridge, Visible light photo-oxidation of model pollutants using $CaCu_{(3)}Ti_{(4)}O_{(12)}$: an experimental and theoretical study of optical properties, electronic structure, and selectivity, J. Am. Chem. Soc. 133 (2011) 1016–1032.
[44] K. Chhor, J.F. Bocquet, C. Colbeau-Justin, Comparative studies of phenol and salicylic acid photocatalytic degradation: influence of adsorbed oxygen, Mater. Chem. Phys. 86 (2004) 123–131.